

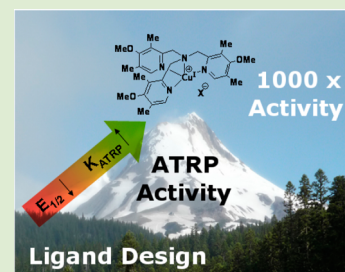
Substituted Tris(2-pyridylmethyl)amine Ligands for Highly Active ATRP Catalysts

Kristin Schröder, Robert T. Mathers, Johannes Buback, Dominik Konkolewicz, Andrew J. D. Magenau, and Krzysztof Matyjaszewski*

Department of Chemistry, Carnegie Mellon University, 4400 Fifth Avenue, Pittsburgh, Pennsylvania 15213, United States

S Supporting Information

ABSTRACT: The synthesis and application of a very active catalyst for copper-catalyzed atom transfer radical polymerizations (ATRP) with tris([(4-methoxy-2,5-dimethyl)-2-pyridyl] methyl)amine (TPMA*) ligand is reported. Catalysts with TPMA* ligands are approximately 3 orders of magnitude more active than those with tris(2-pyridylmethyl)amine (TPMA). Catalyst activity was evaluated by cyclic voltammetry, stopped-flow, and ATRP kinetics. Catalysts with TPMA* ligands perform better than those with TPMA ligands, especially at low catalyst concentrations.



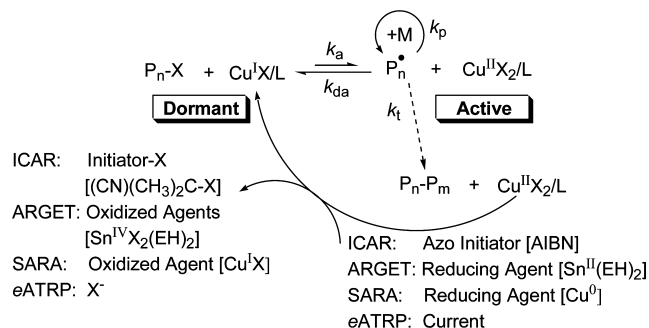
Transition metal catalyzed controlled/living radical polymerization (CRP), that is, organometallic-mediated radical polymerization¹ and atom transfer radical polymerizations (ATRP),² are among the most rapidly developing areas of synthetic chemistry, as they provide polymers with predefined functionalities, compositions, and architectures.³ In the past decade, efficiency of ATRP has been significantly improved, requiring only ppm levels of catalyst in new ATRP procedures⁴ such as activators regenerated by electron transfer (ARGET),⁵ initiators for continuous activators regeneration (ICAR),⁶ electrochemically mediated ATRP (*e*ATRP),⁷ or with zerovalent metals acting as supplemental activators and reducing agents (SARA).⁸ These processes are summarized in Scheme 1, where the activator complex (Cu^IX/L) is (re)-generated in situ from the oxidatively stable deactivator complex (Cu^{II}X₂/L).

Control/living in ATRP is established through a dynamic, rapid, and reversible equilibrium between dormant and active polymerization states, which promote concurrent growth of each polymer chain and mediate the concentration of propagating radicals (P_n^{*}). The ATRP equilibrium constant

(K_{ATRP}), defined as the ratio of activation (k_a) to deactivation (k_{da}) rate constants, is dependent on a variety of reaction parameters including temperature,⁹ pressure,¹⁰ and solvent.¹¹ K_{ATRP} is strongly influenced by the structure and properties of involved chemical components: alkyl halide (R-X, initiator; P_n-X, polymer) and catalyst (Mtⁿ/L, Mt = Cu, Ru, Fe, etc.), each capable of altering K_{ATRP} over 6 orders of magnitude.¹²

The rational design of ligands using established structure–activity relationships provides a promising strategy to develop superior catalytic systems to further improve the ATRP process and surpass the current “state-of-the-art” ATRP systems. Presently, tris[2-(dimethylamino)ethyl] amine (Me₆TREN)¹³ and tris(2-pyridylmethyl)amine (TPMA)¹⁴ represent the most active and commonly employed ligands for ATRP under ppm catalyst concentrations. In ATRP, catalyst activity has been correlated with ligand denticity, chelating effects, type of N-donor atoms, and ligand structure.^{12b} Also, electron donating groups (EDGs) in *para*-substituted 2,2'-bipyridine ligands profoundly increased ATRP catalyst activity.¹⁵ Therefore, the introduction of EDGs on the even more active TPMA scaffold should provide an amplified improvement in catalytic activity to achieve even larger ATRP equilibrium constants. Similar strategies have been applied to TPMA scaffolds for other catalytic transformations,¹⁶ and their respective Cu^I/L and Cu^{II}/L coordination complexes have been characterized.^{16a,17} Herein, *p*-MeO and *m*-Me groups were incorporated into a TPMA scaffold to enhance the electron donating character and increase ATRP catalyst activity. Hammett sigma constants are -0.07 and -0.27 for methyl $\sigma_m(\text{Me})$ and methoxy $\sigma_p(\text{OMe})$ substituents, respectively.^{15a}

Scheme 1. Mechanism of ppm Cu-Catalyzed ATRP



Received: July 23, 2012

Accepted: July 26, 2012

Published: July 30, 2012

Table 1. ARGET and SARA ATRP of *n*-Butyl Acrylate and Methyl Acrylate

entry ^a	[M]/[I]	[Sn(EH) ₂]	cat. loading ^b (ppm)	T (°C)	t (h)	conv. (%)	M _{n,GPC}	M _{n,theo} ^c	M _w /M _n
1	160	0.1	50	60	21	80	16600	16400	1.16
2 ^d	160	0.1	50	60	21	60	14400	12300	1.12
3	160	0.2	100	60	5.16	72	11000	15800	1.15
4	160	0.2	100	60	21	91	20100	18900	1.09
5	160	0.1	50	40	21	70	16000	14600	1.18
6	160	0.05	50	60	21	72	16300	14900	1.16
7 ^e	200		n.d.	25	2	54	10090	9290	1.19
8 ^{d,e}	200		n.d.	25	2	44	9110	7570	1.44

^aARGET ATRP conditions: [BA]/[EBiB]/[Sn(EH)₂]/[TPMA*]/[CuCl₂] = 160:1:0.1:0.03–0.06:0.008–0.016, [BA] = 5.88 M, 20% (v/v) anisole, conversion was determined either by ¹H NMR or gravimetry. ^bMolar ratio of CuCl₂ to monomer. ^cM_{n,theo} = [M]/[I] × conv. × MW_{monomer} + MW_{initiator}. ^dTPMA was used instead of TPMA*. ^eATRP conditions were changed to [MA]/[MBP]/[TPMA*] = 200:1:0.1, [MA] = 7.4 M, with Cu⁰ wire (*d* = 1 mm), 33.3% (v/v) DMSO, T = 25 °C, n.d. = not defined, according to ref 25.

Tris([(4-methoxy-2,5-dimethyl)-2-pyridyl]methyl)amine (herein we use an abbreviated name, TPMA*) was synthesized in a three-step procedure with an overall yield of 30% (Supporting Information (SI), Scheme 1). TPMA* with three EDGs (i.e., 2 × Me and 1 × OMe) on each pyridine moiety provides a total of nine EDGs.

The formation of a coordination complex [Cu^{II}(TPMA)₂] or [Cu^{II}(TPMA)X]₂ in solution was confirmed by electrospray mass spectrometry (ESI-MS) with a [Cu^{II}(TPMA*)Cl]⁺ species in acetonitrile at *m/z* 562.1. CV analysis of TPMA* based complexes shows half-wave potentials (*E*_{1/2}) much more negative than previously reported for ATRP catalysts based on Cu,^{12b,18} Fe,¹⁹ and Ru,²⁰ suggesting larger *K*_{ATRP} values. Cyclic voltammograms in the absence and presence of bromide anions are shown in SI, Figure 1A. The ratios of stability constants of complexation by TPMA* and Br anions for Cu^{II} versus Cu^I (β^{II}/β^I)²¹ are 2.4 × 10²⁰ and 3.6 × 10⁴, respectively, as compared to the unsubstituted TPMA = 3.2 × 10¹⁷ and Br = 2.5 × 10⁴. This indicates much stronger stabilization of the Cu^{II}/L oxidation state by TPMA* relative to TPMA. The *E*_{1/2} value (−0.420 V) determined for Br[−]Cu^{II}/TPMA versus the standard calomel electrode (SCE) is about 120 mV more negative than Me₆TREN and 180 mV more negative than TPMA.^{12b} This suggests a value of *K*_{ATRP} for Cu/TPMA* approximately 3 orders of magnitude larger than for Cu/TPMA, therefore, representing the most active ATRP catalyst developed to date.

The catalytic ability of Cu/TPMA* was initially qualitatively evaluated by CV in the presence of an alkyl halide initiator, that is, ethyl 2-bromoisobutyrate (EBiB; SI, Figure 1B). With EBiB, the cyclic voltammogram showed a dramatically enhanced cathodic current and a greatly diminished anodic current. This type of catalytic response is due to the homogeneous redox reaction between the electrochemically generated Cu^I/TPMA* species and EBiB,²² effectively regenerating Cu^{II}/TPMA* and leading to a greater than one-electron/mol reduction process.

These results were confirmed quantitatively by determining the *K*_{ATRP} of Cu^I/TPMA* via stopped-flow measurements using methyl-2-bromopropionate (MBP) as the initiator in acetonitrile at 25 °C.^{12b} Assuming only activation, deactivation, and termination events take place, *K*_{ATRP} was calculated from the slope (*m*) of a *F*(*Y*) versus time (*t*) plot using the formula *K*_{ATRP} = (*m*/2*k*_t)^{1/2} with *Y* = [Cu^{II}] and *k*_t = 3.5 × 10⁹ M^{−1} s^{−1} for acetonitrile (SI, Figure 2).^{11,23} The *K*_{ATRP} for Cu/TPMA* was determined to be 4.2 × 10^{−4}, which is 1300 times larger than for Cu/TPMA (*K*_{ATRP} = 3.2 × 10^{−7}).^{12b,24} The activation rate coefficient (*k*_{a,TPMA*}) of 8400 M^{−1} s^{−1} was determined by

trapping the generated methyl 2-propionate radicals with 2,2,6,6-tetramethylpiperidyl-1-oxy (TEMPO; SI, Figures 3,4). *k*_{a,TPMA*} was about 2000 times larger than the reported value for Cu/TPMA (*k*_{a,TPMA} = 3.8 M^{−1} s^{−1}).^{12b}

Several ATRP methodologies were investigated to assess the viability of TPMA*. Initially, normal ATRP experiments were conducted with methyl acrylate (MA) and Cu^I/TPMA* in bulk. Despite its high activity, only low conversions and moderate control were observed. After 1 h, the monomer conversion was 7% and the resulting polymers had a high dispersity, *M*_w/*M*_n = 1.34. At longer reaction times, no significant conversion increase was achieved; conversion was only 13.5% after 5.15 h (SI, Table 1). In contrast, the less active Cu/TPMA catalyst reached 79% conversion in about 1 h with a dispersity of 1.05 under identical conditions.¹⁴ This behavior results from the highly active nature of Cu^I/TPMA*, creating high radical concentrations, significant termination, and rapid conversion of Cu^I/TPMA* to X-Cu^{II}/TPMA*. As a result, a strong decrease in the polymerization rate occurred. These results imply that extremely active catalysts are not well suited for traditional ATRP in which the Cu^I/L activator complex cannot be regenerated. Therefore, polymerization systems that continuously regenerate Cu^I/L were explored (ARGET, SARA, ICAR, and *e*ATRP).

First, ARGET and SARA ATRP were investigated under conditions identical to those previously reported.^{5,25} Table 1 summarizes the results for *n*-butyl acrylate (BA) with tin(II) 2-ethylhexanoate (Sn(EH)₂) (entries 1–6) and methyl acrylate (MA) with zerovalent copper (entries 7–8). Under ARGET conditions with 50 ppm of Cu/L, higher conversion and improved correlation between experimental (*M*_{n,exp}) and theoretical molecular weight (*M*_{n,theo}) values were observed with TPMA*, as compared to TPMA ligand (Table 1, entries 1 and 2).

Entries 3 and 4 show the effect of increasing the amount of reducing agent to 0.2 equiv and catalyst (i.e., 100 ppm). Higher concentrations of reducing agent and catalyst revealed an increased rate of polymerization (i.e., higher monomer conversion), excellent correlations between *M*_{n,exp} and *M*_{n,theo} values, and a narrower molecular weight distribution (MWD) compared to the 50 ppm system (entry 1). Decreasing the temperature to 40 °C (entry 5) slightly decreased conversion (Δ = 10%), while maintaining a low dispersity (*M*_w/*M*_n ≈ 1.2). A further decrease of the Sn(EH)₂ concentration to 0.05 equiv (entry 6) and utilizing 50 ppm of catalyst resulted in a controlled polymerization, as evidenced by first-order kinetics and a linear increase in *M*_n with monomer conversion (SI,

Figure 5). TPMA and TPMA* were also investigated with copper wire in SARA ATRP (Table 1, entries 7,8) under conditions similar to those previously reported.²⁵ The Cu^I/TPMA* catalyst resulted in higher conversion and significantly lower dispersity ($M_w/M_n = 1.19$), relative to TPMA ($M_w/M_n = 1.44$).

Next, eATRP was employed for the polymerization of BA at room temperature using 100 ppm of catalyst. In each case, the applied potential (E_{app}) was selected about 80 mV more negative than the cathodic peak potential (E_{pc}) to ensure the rapid reduction of Cu^{II} and a reasonable rate of polymerization. TPMA displayed first-order kinetics below conversion values of 80% and had an apparent rate coefficient (k_{app}) of 0.61 h⁻¹ (SI, Figure 6A). In contrast, TPMA* exhibited an induction period of about 1 h, after which, first-order kinetics were observed with a k_{app} value of 0.91 h⁻¹ (SI, Figures 6A and 7). For both systems, the molecular weight increased linearly with monomer conversion, and low M_w/M_n values were maintained throughout the duration of polymerization (SI, Figure 6B). When comparing the two catalytic systems, TPMA* had improved correlation between $M_{n,exp}$ and $M_{n,theo}$ values and consistently lower M_w/M_n values.

Last, ICAR ATRP was used to evaluate TPMA and TPMA*. The results are summarized in Figures 1 and 2 and in the SI,

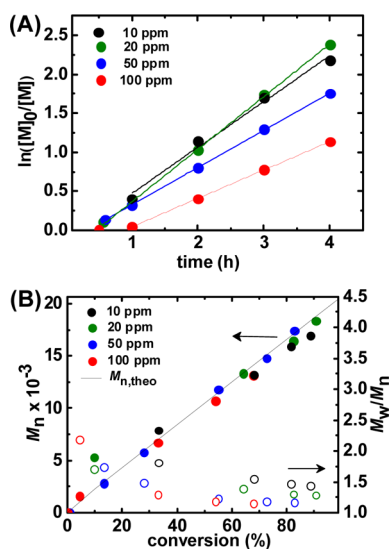


Figure 1. First order kinetic plots (A) and M_n and M_w/M_n as a function of conversion (B); conditions: $[BA]/[EBiB]/[AIBN]/[TPMA^*]/[CuCl_2] = 160:1:0.2:0.006-0.06:0.0016-0.016$, $[BA] = 5.88$ M, 20% (v/v) anisole, $T = 60$ °C.

Table 2 and Figure 8.⁶ Similar to ARGET, SARA, and eATRP, Cu/TPMA* had significantly better performance than Cu/TPMA. The Cu/TPMA* systems displayed nearly ideal ICAR ATRP behavior when changing the catalyst concentration.²⁶ In each case, linear first-order kinetic plots were obtained, demonstrating constant radical concentrations (Figure 1A and SI, Figure 9B). These plots revealed k_{app} values of 0.36 h⁻¹ (100 ppm), 0.48 h⁻¹ (50 ppm), 0.68 h⁻¹ (20 ppm), 0.59 h⁻¹ (10 ppm), and 0.82 h⁻¹ (5 ppm). In addition, all the ICAR systems produced polymers with low dispersities, confirming controlled polymerizations (Figure 1B). Higher catalyst loadings decreased the dispersities of the resulting polymers with $M_w/M_n = 1.50$ and 1.15 at 10 and 100 ppm catalyst, respectively. Despite variations in polymer dispersities, the $M_{n,exp}$ and $M_{n,theo}$ values

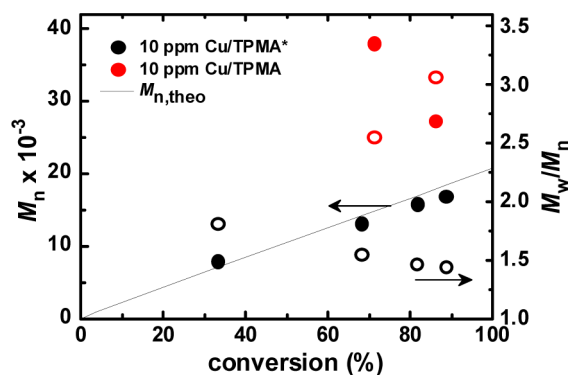


Figure 2. M_n and M_w/M_n as function of conversion for Cu/TPMA and Cu/TPMA* at 10 ppm: $[BA]/[EBiB]/[AIBN]/[TPMA^*]/[CuCl_2] = 160:1:0.2:0.006:0.0016$, $[BA] = 5.88$ M, 20% (v/v) anisole, $T = 60$ °C.

agreed well for all catalyst concentrations between 10 and 100 ppm (Figure 1B).

When comparing TPMA and TPMA* with 5, 10, and 50 ppm catalyst, significant differences in polymerization behavior were observed (SI, Table 2, entries 1–4, 6, and 7). The polymerization rates for both catalysts were comparable at 5 and 10 ppm catalyst concentrations; however, in all cases, ICAR ATRP with Cu/TPMA* resulted in better control than with Cu/TPMA (Figure 2 and SI, Figure 7). Figure 2 directly compares TPMA and TPMA* at 10 ppm catalyst. The Cu/TPMA* system shows linear growth of the molecular weight with conversion, whereas Cu/TPMA shows characteristics resembling conventional radical polymerization, that is, $M_{n,exp} \gg M_{n,theo}$ and broad MWD ($M_w/M_n \approx 3$). With 50 ppm catalyst after 4 h, TPMA* provided polymers with narrower MWD ($M_w/M_n = 1.17$ at 83% conversion) compared to TPMA ($M_w/M_n = 1.67$ at 38% conversion), as shown in SI, Table 2 (entries 6,7).

PREDICI simulations were performed using coefficients obtained from stopped-flow measurements to provide additional insight into normal and ICAR ATRP results. A detailed summary of all simulation parameters are supplied in the SI, Tables 3–7.

Simulation results confirm the poor CRP behavior of normal ATRP (SI, Figure 10) and excellent results for ICAR ATRP (SI, Figure 11). Figure 10A,B of the SI reinforces the hypothesis that Cu^I was rapidly converted to Cu^{II} and limited conversions with highly active catalysts (i.e., TPMA*) in normal ATRP. In contrast, the less reactive TPMA demonstrated better performance, as shown in the experimental results. PREDICI simulations for ICAR ATRP illustrated the opposite behavior for TPMA and TPMA*. The TPMA* system exhibited characteristics of CRP (i.e., first-order kinetics and low M_w/M_n values), whereas TPMA proceeded in an uncontrolled fashion (SI, Figure 11A,B). Better control was achieved with TPMA* under low catalyst concentrations, because the large K_{ATRP} values of TPMA* provide a sufficiently high $[Cu^{II}/L]$. As shown in SI, Figure 11C, the Cu^{II}/Cu_{tot} ratio remains constant and high for TPMA*, whereas it decreases rapidly for TPMA. Systems containing larger absolute $[Cu^{II}]$ provide polymers with lower M_w/M_n values (SI, Figure 11B).

In conclusion, a very active ATRP catalyst was prepared with TPMA containing nine EDGs. The highly active nature of Cu^I/TPMA* was confirmed by CV, stopped-flow measurements, and via kinetic analysis of both experimental and simulated polymerizations. CV and stopped-flow kinetic measurements

revealed $\text{Cu}^{\text{I}}/\text{TPMA}^*$ to be 3 orders of magnitude more active than $\text{Cu}^{\text{I}}/\text{TPMA}$. ATRP of acrylates with $\text{Cu}^{\text{I}}/\text{TPMA}^*$ were more successful with ppm catalyst systems (ARGET, ICAR, SARA, and eATRP) than in normal ATRP. Other derivatives of TPMA^* are envisioned to even further increase K_{ATRP} and eventually grant access to less reactive monomers (i.e., vinyl acetate, etc.) in ATRP.

■ ASSOCIATED CONTENT

● Supporting Information

Experimental details and additional figures and tables. This material is available free of charge via the Internet at <http://pubs.acs.org>.

■ AUTHOR INFORMATION

Corresponding Author

*E-mail: km3b@andrew.cmu.edu.

Notes

The authors declare no competing financial interest.

■ ACKNOWLEDGMENTS

The authors would like to thank the CRP Consortium at Carnegie Mellon University and NSF (CHE-1026060, CHE-1039870, CHE-0130903, DBI-9729351) for financial support. K.S. thanks the Deutsche Forschungsgemeinschaft (DFG) for her postdoctoral fellowship.

■ REFERENCES

- (1) (a) Poli, R. *Angew. Chem., Int. Ed.* **2006**, *45*, 5058. (b) Poli, R. *Eur. J. Inorg. Chem.* **2011**, *2011*, 1513.
- (2) (a) Kamigaito, M.; Ando, T.; Sawamoto, M. *Chem. Rev.* **2001**, *101*, 3689. (b) Matyjaszewski, K.; Xia, J. H. *Chem. Rev.* **2001**, *101*, 2921. (c) di Lena, F.; Matyjaszewski, K. *Prog. Polym. Sci.* **2010**, *35*, 959.
- (3) (a) Tsarevsky, N. V.; Matyjaszewski, K. *Chem. Rev.* **2007**, *107*, 2270. (b) Matyjaszewski, K. *Macromolecules* **2012**, *45*, 4015. (c) Matyjaszewski, K.; Spanswick, J., Copper-Mediated Atom Transfer Radical Polymerization. In *Polymer Science: A Comprehensive Reference*; Matyjaszewski, K., Möller, M., Eds.; Elsevier BV: Amsterdam, 2012; Vol. 3, p 377. (d) Matyjaszewski, K.; Tsarevsky, N. V. *Nat. Chem.* **2009**, *1*, 276.
- (4) Pintauer, T.; Matyjaszewski, K. *Chem. Soc. Rev.* **2008**, *37*, 1087.
- (5) Jakubowski, W.; Matyjaszewski, K. *Angew. Chem., Int. Ed.* **2006**, *45*, 4482.
- (6) Matyjaszewski, K.; Jakubowski, W.; Min, K.; Tang, W.; Huang, J.; Braunecker, W. A.; Tsarevsky, N. V. *Proc. Natl. Acad. Sci. U.S.A.* **2006**, *103*, 15309.
- (7) (a) Magenau, A. J. D.; Strandwitz, N. C.; Gennaro, A.; Matyjaszewski, K. *Science* **2011**, *332*, 81. (b) Bortolamei, N.; Isse, A. A.; Magenau, A. J. D.; Gennaro, A.; Matyjaszewski, K. *Angew. Chem., Int. Ed.* **2011**, *50*, 11391.
- (8) (a) Min, K.; Gao, H. F.; Matyjaszewski, K. *J. Am. Chem. Soc.* **2005**, *127*, 3825. (b) Percec, V.; Guliasvili, T.; Ladislav, J. S.; Wistrand, A.; Stjernedahl, A.; Sienkowska, M. J.; Monteiro, M. J.; Sahoo, S. *J. Am. Chem. Soc.* **2006**, *128*, 14156. (c) Matyjaszewski, K.; Tsarevsky, N. V.; Braunecker, W. A.; Dong, H.; Huang, J.; Jakubowski, W.; Kwak, Y.; Nicolay, R.; Tang, W.; Yoon, J. A. *Macromolecules* **2007**, *40*, 7795. (d) Zhang, Y.; Wang, Y.; Matyjaszewski, K. *Macromolecules* **2011**, *44*, 683.
- (9) Seeliger, F.; Matyjaszewski, K. *Macromolecules* **2009**, *42*, 6050.
- (10) Morick, J.; Buback, M.; Matyjaszewski, K. *Macromol. Chem. Phys.* **2011**, *212*, 2423.
- (11) Braunecker, W. A.; Tsarevsky, N. V.; Gennaro, A.; Matyjaszewski, K. *Macromolecules* **2009**, *42*, 6348.
- (12) (a) Tang, W.; Matyjaszewski, K. *Macromolecules* **2006**, *39*, 4953. (b) Tang, W.; Kwak, Y.; Braunecker, W.; Tsarevsky, N. V.; Coote, M. L.; Matyjaszewski, K. *J. Am. Chem. Soc.* **2008**, *130*, 10702.
- (13) Xia, J.; Gaynor, S. G.; Matyjaszewski, K. *Macromolecules* **1998**, *31*, 5958.
- (14) Xia, J.; Matyjaszewski, K. *Macromolecules* **1999**, *32*, 2434.
- (15) (a) Hansch, C.; Leo, A.; Taft, R. W. *Chem. Rev.* **1991**, *91*, 165. (b) Magenau, A. J. D.; Kwak, Y.; Schröder, K.; Matyjaszewski, K. *ACS Macro Lett.* **2012**, 508.
- (16) (a) Zhang, C. X.; Kaderli, S.; Costas, M.; Kim, E.-i.; Neuhold, Y.-M.; Karlin, K. D.; Zuberbühler, A. D. *Inorg. Chem.* **2003**, *42*, 1807. (b) Xue, G.; Wang, D.; De Hont, R.; Fiedler, A. T.; Shan, X.; Münck, E.; Que, L. *Proc. Natl. Acad. Sci. U.S.A.* **2007**, *104*, 20713. (c) Maiti, D.; Fry, H. C.; Woertink, J. S.; Vance, M. A.; Solomon, E. I.; Karlin, K. D. *J. Am. Chem. Soc.* **2006**, *129*, 264.
- (17) (a) Eckenhoff, W. T.; Pintauer, T. *Inorg. Chem.* **2010**, *49*, 10617. (b) Bonniard, L.; de la Lande, A.; Ulmer, S.; Piquemal, J.-P.; Parisel, O.; Gérard, H. *Catal. Today* **2011**, *177*, 79.
- (18) Qiu, J.; Matyjaszewski, K.; Thouin, L.; Amatore, C. *Macromol. Chem. Phys.* **2000**, *201*, 1625.
- (19) O'Reilly, R. K.; Gibson, V. C.; White, A. J. P.; Williams, D. J. *J. Am. Chem. Soc.* **2003**, *125*, 8450.
- (20) Ando, T.; Kamigaito, M.; Sawamoto, M. *Macromolecules* **2000**, *33*, 5825.
- (21) Bortolamei, N.; Isse, A. A.; Di Marco, V. B.; Gennaro, A.; Matyjaszewski, K. *Macromolecules* **2010**, *43*, 9257.
- (22) Isse, A. A.; Gennaro, A. *J. Phys. Chem. A* **2004**, *108*, 4180.
- (23) Tang, W.; Tsarevsky, N. V.; Matyjaszewski, K. *J. Am. Chem. Soc.* **2006**, *128*, 1598.
- (24) (a) Note that, in ref 12b, the value of $k_t = 2.5 \times 10^9 \text{ M}^{-1} \text{ s}^{-123}$ was used to calculate K_{ATRP} for $\text{Cu}^{\text{I}}/\text{TPMA}$, leading to $K_{\text{ATRP}} = 3.7 \times 10^{-7}$. Instead, we used here the experimental value of $k_t = 3.5 \times 10^9 \text{ M}^{-1} \text{ s}^{-1,11}$ yielding $K_{\text{ATRP}} = 3.2 \times 10^{-7}$. (b) Fischer, H.; Radom, L. *Angew. Chem., Int. Ed.* **2001**, *40*, 1340.
- (25) Zhang, Y.; Wang, Y.; Peng, C.-h.; Zhong, M.; Zhu, W.; Konkolewicz, D.; Matyjaszewski, K. *Macromolecules* **2011**, *45*, 78.
- (26) D'Hooge, D. R.; Konkolewicz, D.; Reyniers, M.-F.; Marin, G. B.; Matyjaszewski, K. *Macromol. Theor. Simul.* **2012**, *21*, 52.